A factor graph approach to digital self-interference mitigation in OFDM full-duplex systems

Frederic Lehmann and A. O. Berthet

***Abstract*—Digital self-interference cancellation is a major challenge for OFDM full-duplex transmissions. Therefore, reliable estimation of both the signal-of-interest and the self-interference channel, becomes the limiting factor in a mobile radio context. In this paper, improved estimation of the time-varying channels is obtained by solving the problem jointly with self-interference cancellation and decoding using a factor graph approach. Taking advantage of the per-subcarrier structure of message-passing, a low-complexity receiver is obtained. Our semi-analytical and numerical results show the superiority of the proposed scheme over state-of-the art self-interference cancellation methods under limited pilot overhead.**

***Index Terms*—OFDM, full-duplex, self-interference mitigation, joint channel estimation and decoding, message-passing receiver.**

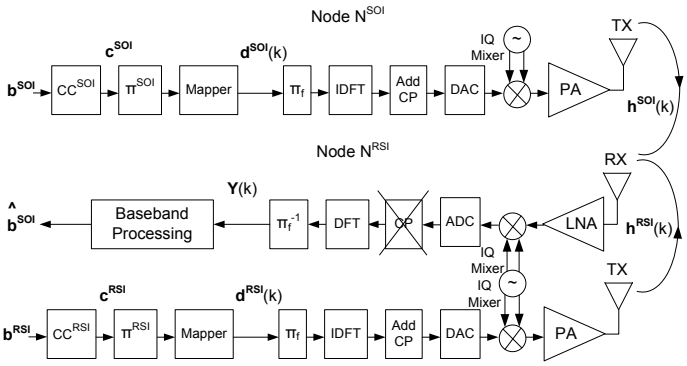

Fig. 1. Architecture of the OFDM-based nodes: near-end node (N^{RSI}), and far-end node (N^{SOI}).

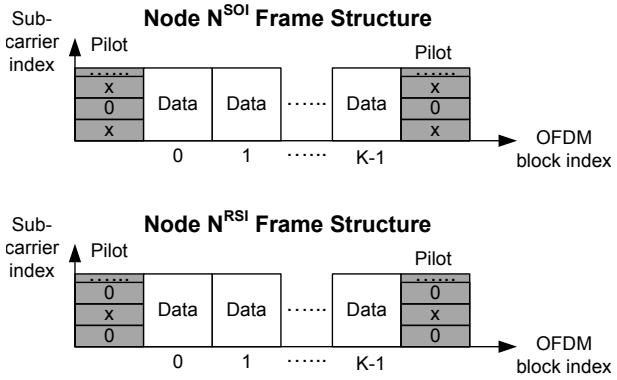

Fig. 2. Frame structure including: pilot blocks (shaded) and data blocks (unshaded). In a pilot block, a 0 (resp. an x) denotes a silent (resp. an active) subcarrier.

I. Introduction

Full-duplex (FD) wireless communications have the potential to double the ergodic capacity with respect to (wrt) conventional half-duplex (HD) systems [1]. Since the capacity increase of FD communications is obtained by allowing simultaneous transmission and reception over the same frequency band, the high level of self-interference (SI) at the receiver side is drowning out the signal-of-interest (SOI). Consequently, SI cancellation has attracted a lot of attention in the recent literature [1]. Passive methods rely on isolation/shielding of the transmit and receive antennas, while active methods mainly rely on analog domain SI cancellation to avoid saturation of the analog-to-digital converter (ADC). After combined passive and active analog cancellation, the residual self-interference (RSI) must be cancelled down to the noise floor.

The focus of this paper is on digital domain RSI cancellation for OFDM FD transceivers equipped with one transmit and one receive antenna. Previous studies have considered RSI channel estimation, followed by RSI reconstruction from the known SI data (in the time or frequency domain) and cancellation. First, least squares (LS) estimation of the RSI channel impulse response (CIR) has been used in [2] and [3] to mitigate linear and nonlinear effects, respectively. Since the presence of the SOI is ignored, several consecutive OFDM blocks are needed to obtain reliable LS estimates. Second, using orthogonal pilot symbols for the SI and SOI, channel frequency response (CFR) estimation is advocated in [4] and [5] to mitigate linear and nonlinear effects, respectively. Assuming one pilot per channel coherence time, the estimated parameters are then used during subsequent OFDM data blocks.

Against this background, the main contribution of this paper is to introduce a RSI mitigation scheme for fast-moving devices, where the channel can vary from one OFDM block to the next. The proposed low complexity receiver performs joint RSI/SOI channel estimation, RSI cancellation and decoding, based on a factor graph approach. The key ingredient is that that both the pilot and data OFDM blocks serve the purpose of RSI mitigation in the presence of nonlinear effects.

Throughout the paper, bold letters indicate vectors and matrices, while $\mathbf{0}_{m\times n}$ is the $m\times n$ all-zero matrix and $\mathrm{diag}\{\mathbf{a}\}$ is the diagonal matrix, whose diagonal entries are stored in vector $\mathbf{a}$ and whose off-diagonal entries are zero. The circular convolution operator is denoted by $\circledast$. $\mathcal{N}_{\mathcal{C}}(\mathbf{x}:\mathbf{m},\mathbf{P})$ denotes a complex Gaussian distribution of the variable $\mathbf{x}$, with mean $\mathbf{m}$ and covariance matrix $\mathbf{P}$.

F. Lehmann is with SAMOVAR, Télécom SudParis, CNRS, Université Paris-Saclay, 9 rue Charles Fourier 91011 EVRY, France (e-mail: frederic.lehmann@it-sudparis.eu).

A. O. Berthet is with L2S, Centrale Supélec, CNRS, Université Paris-Saclay, Plateau de Moulon, 3 rue Joliot Curie 91192 GIF-SUR-YVETTE, France (e-mail: antoine.berthet@centralesupelec.fr).

II. System model

We consider the receiver chain of a full-duplex node $\mathsf{N}^{\mathsf{RSI}}$ equipped with one transmit and one receive antenna, attempting to detect, under RSI originating from the transmit chain of that same node, the weak far-field SOI from node $\mathsf{N}^{\mathsf{SOI}}$, as depicted in Fig. 1.

A. Transceiver structure

We propose the bit-interleaved coded modulation (BICM)-based transceiver of Fig. 1. Node N^q, $q \in \{\mathsf{RSI}, \mathsf{SOI}\}$ generates a sequence of independently and uniformly distributed binary digits $\mathbf{b}^q$. Then the convolutional encoder CC^q producing the coded vector $\mathbf{c}^q$, is followed by a bit-interleaver $\pi^q(.)$ and a symbol mapper, which produces complex modulated symbols for a frame of K consecutive OFDM data blocks using N subcarriers. Let $\mathbf{d}^q(k) = [d_0^q(k), \ldots, d_{N-1}^q(k)]^T$ be the N modulated symbols corresponding to k-th OFDM data block sent by N^q, with unit energy so that $E[|d_n^q(k)|^2] = 1$, $\forall(q, n, k)$. The time domain OFDM signal is obtained by feeding $\sqrt{E_s^q}\mathbf{d}^q(k)$ to a frequency interleaver $\pi_f(.)$, then to a length-N IDFT, before appending a length-Δ cyclic prefix, where E_s^q is the energy per symbol for the signal transmitted by N^q. At the beginning and at the end of each frame, $\mathsf{N}^{\mathsf{RSI}}$ and $\mathsf{N}^{\mathsf{SOI}}$ append pilot OFDM blocks, that are orthogonal in the frequency domain as depicted in Fig. 2. To support wireless full-duplex communications, we assume timing synchronization between the near-end and the far-end node [6].

B. Residual self-interference model

We assume state-of-the-art combined passive and active analog cancellation, so that only RSI needs to be cancelled in the digital domain. Following [7], we assume that the quantization noise is much smaller than the thermal noise, the in-phase/quadrature (IQ) imbalance can be calibrated and the low-noise amplifier (LNA) at the receiver antenna is operated in the linear regime. Therefore, RF component imperfections are dominated by transmit power amplifier (PA) nonlinearities. Without loss of generality, consider the discrete-time signal for the k-th OFDM block before the PA at N^{RSI}

$$s_t(k) = \frac{\sqrt{E_s^{\mathsf{RSI}}}}{\sqrt{N}} \sum_{n=0}^{N-1} d_{\pi_f(n)}^{\mathsf{RSI}}(k) e^{j\frac{2\pi nt}{N}}, \ -\Delta \leq t \leq N-1. \tag{1}$$

The output of the nonlinear PA can be modeled using a third-order memory-Q Hammerstein model (HM) as [3]

$$\{y_t(k)\} = \boldsymbol{\alpha}^1 \circledast \{s_t(k)\} + \boldsymbol{\alpha}^3 \circledast \{s_t(k)|s_t(k)|^2\}, \tag{2}$$

where $\boldsymbol{\alpha}^1$ (resp. $\boldsymbol{\alpha}^3$) is the length-Q impulse response corresponding to the linear (resp. nonlinear) part of the HM. The generalization to higher order HMs is straightforward. Let $\mathbf{h}^{\mathsf{RSI}}(k)$ denote the length-L RSI CIR, the received noiseless time-domain RSI signal for the k-th OFDM block after CP suppression, has the form

$$\{z_t(k)\} = \mathbf{c}^{\mathsf{RSI}}(k) \circledast \{s_t(k)\} + \mathbf{g}^{\mathsf{RSI}}(k) \circledast \{s_t(k)|s_t(k)|^2\}, \tag{3}$$

where $\mathbf{c}^{\mathsf{RSI}}(k) = \mathbf{h}^{\mathsf{RSI}}(k) * \boldsymbol{\alpha}^1$, $\mathbf{g}^{\mathsf{RSI}}(k) = \mathbf{h}^{\mathsf{RSI}}(k) * \boldsymbol{\alpha}^3$ are length-$(L+Q-1)$ compound CIRs. The corresponding CFRs $\{C_n^{\mathsf{RSI}}(k)\}_{n=0}^{N-1}$ and $\{G_n^{\mathsf{RSI}}(k)\}_{n=0}^{N-1}$ are the zero-padded N-point DFT of $\mathbf{c}^{\mathsf{RSI}}(k)$ and $\mathbf{g}^{\mathsf{RSI}}(k)$, respectively. Note that inter-block interference (IBI) is eliminated when $\Delta \geq L + Q - 1$. Let us also define the modified linear RSI CFR as [8]

$$\tilde{C}_n^{\mathsf{RSI}}(k) = \sqrt{E_s^{\mathsf{RSI}}} \left(C_n^{\mathsf{RSI}}(k) + \frac{G_n^{\mathsf{RSI}}(k)}{N} \sum_{t=0}^{N-1} |s_t(k)|^2 \right) \tag{4}$$

and the inter-carrier interference (ICI) affecting the n-th subcarrier before frequency deinterleaving, as [8]

$$\begin{aligned} ICI_n^{\mathsf{RSI}}(k) = &\frac{1}{\sqrt{N}} \sum_{t=0}^{N-1} s_t(k)|s_t(k)|^2 e^{-j\frac{2\pi nt}{N}} \\ &- \sqrt{E_s^{\mathsf{RSI}}} d_{\pi_f(n)}^{\mathsf{RSI}}(k) \frac{1}{N} \sum_{t=0}^{N-1} |s_t(k)|^2. \end{aligned} \tag{5}$$

The received RSI contribution in the frequency domain during the k-th OFDM block, obtained by applying an N-point DFT to (3) on the n-th subcarrier before frequency deinterleaving, has the form [8]

$$Z_n(k) = d_{\pi_f(n)}^{\mathsf{RSI}}(k) \tilde{C}_n^{\mathsf{RSI}}(k) + ICI_n^{\mathsf{RSI}}(k) G_n^{\mathsf{RSI}}(k), \tag{6}$$

where the first (resp. second) term accounts for the desired component (resp. the nonlinearity-induced ICI). Note that in the absence of nonlinearity, $\mathbf{g}^{\mathsf{RSI}}$ is the all-zero vector, so that the (6) boils down to an ICI-free transmission enabled by subcarrier orthogonality.

C. Observation model

We consider the frequency-domain signal for the k-th OFDM data block $\mathbf{Y}(k) = [Y_0(k), \ldots, Y_{N-1}(k)]^T$, obtained after CP removal, N-point DFT and frequency deinterleaving. Using the far-field assumption, the weak SOI's PA nonlinearities are well below the receiver thermal noise level, so that a length-L CIR $\mathbf{h}^{\mathsf{SOI}}(k)$ is in order for the $\mathsf{N}^{\mathsf{SOI}}$ to $\mathsf{N}^{\mathsf{RSI}}$ channel model during the k-th OFDM block. We let $\tilde{\mathbf{c}}^{\mathsf{SOI}}(k) = \sqrt{E_s^{\mathsf{SOI}}}\mathbf{h}^{\mathsf{SOI}}(k) * \boldsymbol{\alpha}^1$ and $\{\tilde{C}_n^{\mathsf{SOI}}(k)\}_{n=0}^{N-1}$ denote the corresponding compound CIR and CFR, respectively. From (6), after frequency deinterleaving we obtain the observation on the n-th subcarrier during the k-th frame as

$$\begin{cases} \mathbf{H}_n(k) = [d_n^{\mathsf{RSI}}(k), ICI_{\pi_f^{-1}(n)}^{\mathsf{RSI}}(k), d_n^{\mathsf{SOI}}(k)] \\ \mathbf{x}_n(k) = [\tilde{C}_{\pi_f^{-1}(n)}^{\mathsf{RSI}}(k), G_{\pi_f^{-1}(n)}^{\mathsf{RSI}}(k), \tilde{C}_{\pi_f^{-1}(n)}^{\mathsf{SOI}}(k)]^T \\ Y_n(k) = \mathbf{H}_n(k)\mathbf{x}_n(k) + N_n(k), \end{cases} \tag{7}$$

where $\mathbf{H}_n(k)$ is the data-dependent observation matrix, $\mathbf{x}_n(k)$ is the unknown CFR state vector and $N_n(k) \sim \mathcal{N}_C(N_n(k) : 0, N_0)$ denotes the independently distributed thermal noise contribution.

D. State-space model

Assuming perfect frequency interleaving, we adopt an independent Gauss-Markov model for the CFR time-variations on each subcarrier [9]

$$\mathbf{x}_n(k) = \mathbf{x}_n(k-1) + \boldsymbol{\Delta}_n(k), \tag{8}$$

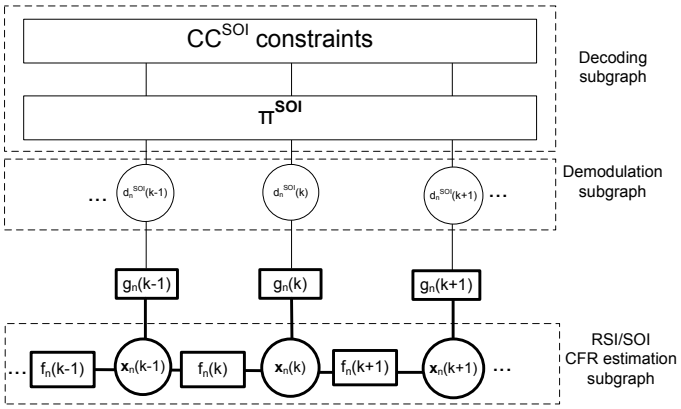

Fig. 3. Factor graph corresponding to n-th subcarrier receiver processing at the near-end node $\mathsf{N}^{\mathsf{RSI}}$.

with a driving noise $\mathbf{\Delta}_n(k) \sim \mathcal{N}_C(\mathbf{\Delta}_n(k) : \mathbf{0}_{3\times 1}, \mathbf{Q})$, where $\mathbf{Q} = \text{diag}\{[q_{\tilde{C}}^{\mathsf{RSI}}, q_G^{\mathsf{RSI}}, q_{\tilde{C}}^{\mathsf{SOI}}]\}$. Since in general (8) only approximates the true state dynamics, we choose the hyperparameters as

$$\begin{cases} q_{\tilde{C}}^{\mathsf{RSI}} = \zeta E\left[|\tilde{C}^{\mathsf{RSI}}_{\pi_f^{-1}(n)}(k) - \tilde{C}^{\mathsf{RSI}}_{\pi_f^{-1}(n)}(k-1)|^2\right] \\ q_G^{\mathsf{RSI}} = \zeta E\left[|G^{\mathsf{RSI}}_{\pi_f^{-1}(n)}(k) - G^{\mathsf{RSI}}_{\pi_f^{-1}(n)}(k-1)|^2\right] \\ q_C^{\mathsf{SOI}} = \zeta E\left[|\tilde{C}^{\mathsf{SOI}}_{\pi_f^{-1}(n)}(k) - \tilde{C}^{\mathsf{SOI}}_{\pi_f^{-1}(n)}(k-1)|^2\right], \end{cases} \quad (9)$$

where ζ is a real parameter in general different from 1, to be optimized in Sec. IV.

E. Factor graph representation

Let $\mathbf{D}^{\mathsf{RSI}} = \{\mathbf{d}^{\mathsf{RSI}}(k)\}_{k=0}^{K-1}$, $\mathbf{D}^{\mathsf{SOI}} = \{\mathbf{d}^{\mathsf{SOI}}(k)\}_{k=0}^{K-1}$, $\mathbf{X} = \{\{\mathbf{x}_n(k)\}_{n=0}^{N-1}\}_{k=0}^{K-1}$ and $\mathbf{Y} = \{\mathbf{Y}(k)\}_{k=0}^{K-1}$. Using Bayes' rule, we factorize the joint *a posteriori* distribution of the SOI data and the CFR channel states as

$$\begin{aligned} &p\left(\mathbf{X}, \mathbf{D}^{\mathsf{SOI}}, \mathbf{c}^{\mathsf{SOI}}, \mathbf{b}^{\mathsf{SOI}} | \mathbf{Y}, \mathbf{D}^{\mathsf{RSI}}\right) \\ &\propto p\left(\mathbf{Y}|\mathbf{X}, \mathbf{D}^{\mathsf{SOI}}, \mathbf{D}^{\mathsf{RSI}}\right) p\left(\mathbf{X}\right) p\left(\mathbf{D}^{\mathsf{SOI}}|\mathbf{c}^{\mathsf{SOI}}\right) p\left(\mathbf{c}^{\mathsf{SOI}}|\mathbf{b}^{\mathsf{SOI}}\right) p(\mathbf{b}^{\mathsf{SOI}}). \end{aligned} \quad (10)$$

Since subcarrier orthogonality is preserved conditional on the known $\mathsf{N}^{\mathsf{RSI}}$ symbols, the first term in the second line of (10) has the form

$$\prod_{n=0}^{N-1}\left\{\prod_{k=0}^{K-1} p(Y_n(k)|\mathbf{x}_n(k), d_n^{\mathsf{SOI}}(k), \mathbf{D}^{\mathsf{RSI}})\right\}.$$

Now, exploiting the first-order Markov property of (8) and assuming that $\pi_f(.)$ implements ideal frequency interleaving, the second term in the second line of (10) can be factorized as

$$\prod_{n=0}^{N-1}\left\{p(\mathbf{x}_n(0))\prod_{k=1}^{K-1} p(\mathbf{x}_n(k)|\mathbf{x}_n(k-1))\right\}.$$

Now, defining the function nodes

$$\begin{aligned} f_n(k) &= p(\mathbf{x}_n(k)|\mathbf{x}_n(k-1)) \\ g_n(k) &= p(Y_n(k)|\mathbf{x}_n(k), d_n^{\mathsf{SOI}}(k), \mathbf{D}^{\mathsf{RSI}}), \end{aligned} \quad (11)$$

(10) can be represented by the factor graph [10] of Fig. 3, where only the n-th subcarrier variables and function nodes are represented for simplicity.

III. Proposed iterative receiver

We apply the sum-product algorithm (SPA) [10], parameterizing all continuous-valued messages by complex Gaussian distributions to obtain a tractable complexity. We let $\mu_{u\to v}(.)$ denote the message sent by node u to node v in the factor graph. SPA on the decoding and demodulation subgraphs, delivers extrinsic symbol probabilities $\mu_{d_n^{\mathsf{SOI}}(k)\to g_n(k)}(d_n^{\mathsf{SOI}}(k))$. After proper normalization, i.e. $\sum_{d_n^{\mathsf{SOI}}(k)} \mu_{d_n^{\mathsf{SOI}}(k)\to g_n(k)}(d_n^{\mathsf{SOI}}(k)) = 1$, we obtain the soft-decision on the n-th subcarrier symbol for the SOI during the k-th block, as $\hat{d}_n^{\mathsf{SOI}}(k) = \sum_{d_n^{\mathsf{SOI}}(k)} \mu_{d_n^{\mathsf{SOI}}(k)\to g_n(k)}(d_n^{\mathsf{SOI}}(k)) d_n^{\mathsf{SOI}}(k)$. Then, the likelihood of observation $Y_n(k)$ given the CFR state $\mathbf{x}_n(k)$,

$$\begin{aligned} &\mu_{g_n(k)\to\mathbf{x}_n(k)}(\mathbf{x}_n(k)) \\ &\propto \sum_{d_n^{\mathsf{SOI}}(k)} \mu_{d_n^{\mathsf{SOI}}(k)\to g_n(k)}(d_n^{\mathsf{SOI}}(k)) p\left(Y_n(k)|\mathbf{x}_n(k), d_n^{\mathsf{SOI}}(k), \mathbf{D}^{\mathsf{RSI}}\right), \end{aligned}$$

is a Gaussian mixture, that we collapse to a single Gaussian using moment-matching

$$\mu_{g_n(k)\to\mathbf{x}_n(k)}(\mathbf{x}_n(k)) \propto \mathcal{N}_C(Y_n(k) : \hat{\mathbf{H}}_n(k)\mathbf{x}_n(k), S_n(k))$$

where

$$\begin{cases} \hat{\mathbf{H}}_n(k) = [d_n^{\mathsf{RSI}}(k), ICI^{\mathsf{RSI}}_{\pi_f^{-1}(n)}(k), \hat{d}_n^{\mathsf{SOI}}(k)] \\ S_n(k) = N_0 + E[|\tilde{C}^{\mathsf{SOI}}_{\pi_f^{-1}(n)}(k)|^2] \\ \qquad\qquad \times \sum_{d_n^{\mathsf{SOI}}(k)} \mu_{d_n^{\mathsf{SOI}}(k)\to g_n(k)}(d_n^{\mathsf{SOI}}(k))|d_n^{\mathsf{SOI}}(k) - \hat{d}_n^{\mathsf{SOI}}(k)|^2. \end{cases}$$

It follows that the forward and backward messages on the CFR estimation subgraph having the form

$$\begin{aligned} &\mu_{f_n(k)\to\mathbf{x}_n(k)}(\mathbf{x}_n(k)) \\ &\propto \mathcal{N}_C(\mathbf{x}_n(k) : \hat{\mathbf{x}}_n(k|k-1), \mathbf{P}_n(k|k-1)) \\ &\mu_{f_n(k+1)\to\mathbf{x}_n(k)}(\mathbf{x}_n(k)) \\ &\propto \mathcal{N}_C(\mathbf{x}_n(k) : \hat{\mathbf{x}}_n(k|k+1:K-1), \mathbf{P}_n(k|k+1:K-1)) \end{aligned}$$

are updated recursively with a Kalman filter and their product

$$\mu_{\mathbf{x}_n(k)\to g_n(k)}(\mathbf{x}_n(k)) \propto \mathcal{N}_C(\mathbf{x}_n(k) : \hat{\mathbf{x}}_n(k \setminus k), \mathbf{P}_n(k \setminus k)), \quad (12)$$

has the mean and covariance corresponding to the two-filter smoothing formula for CFR state estimates

$$\begin{cases} \mathbf{P}_n(k \setminus k) = \mathbf{P}_n(k|k-1)\left[\mathbf{P}_n(k|k-1)) + \mathbf{P}_n(k|k+1:K-1)\right]^{-1} \\ \qquad\qquad \times \mathbf{P}_n(k|k+1:K-1) \\ \hat{\mathbf{x}}_n(k \setminus k) = \mathbf{P}_n(k \setminus k)[\mathbf{P}_n(k|k-1)^{-1}\hat{\mathbf{x}}_n(k|k-1) + \\ \qquad\qquad \mathbf{P}_n(k|k+1:K-1)^{-1}\hat{\mathbf{x}}_n(k|k+1:K-1)]. \end{cases}$$

$k \setminus k$ is used to denote the expectation and covariance of $\mathbf{x}_n(k)$ given $Y_n(0), \ldots, Y_n(k-1), Y_n(k+1), \ldots, Y_n(K-1)$. Finally, using (7) and (12), soft demodulation is obtained as

$$\begin{aligned} &\mu_{g_n(k)\to d_n^{\mathsf{SOI}}(k)}(d_n^{\mathsf{SOI}}(k)) \\ &\propto \int \mu_{\mathbf{x}_n(k)\to g_n(k)}(\mathbf{x}_n(k)) p\left(Y_n(k)|\mathbf{x}_n(k), d_n^{\mathsf{SOI}}(k), \mathbf{D}^{\mathsf{RSI}}\right) d\mathbf{x}_n(k) \\ &\propto \mathcal{N}_C(Y_n(k) : \mathbf{H}_n(k)\hat{\mathbf{x}}_n(k \setminus k), \mathbf{H}_n(k)\mathbf{P}_n(k \setminus k)\mathbf{H}_n(k)^H + N_0). \end{aligned}$$

The SPA on the decoder (resp. demodulator) subgraph is implemented using the BCJR algorithm [11] (resp. classical soft-decision). The proposed method is initialized with uniformly

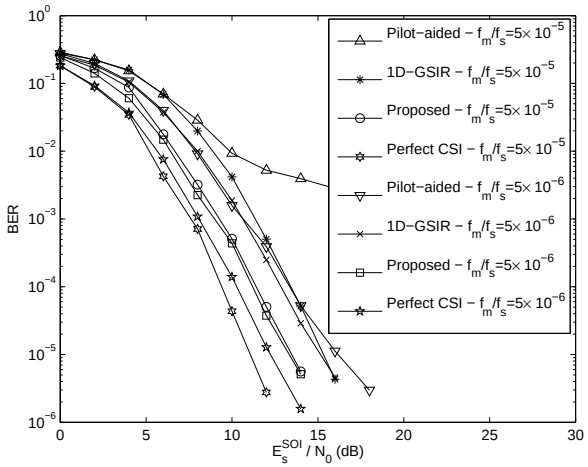

Fig. 4. BER using 4-QAM modulation under varying fading rate for the pilot-aided, 1D-GSIR, proposed and perfect CSI methods after 3 iterations ($\theta_{rms} = 1\,\mathrm{deg}$).

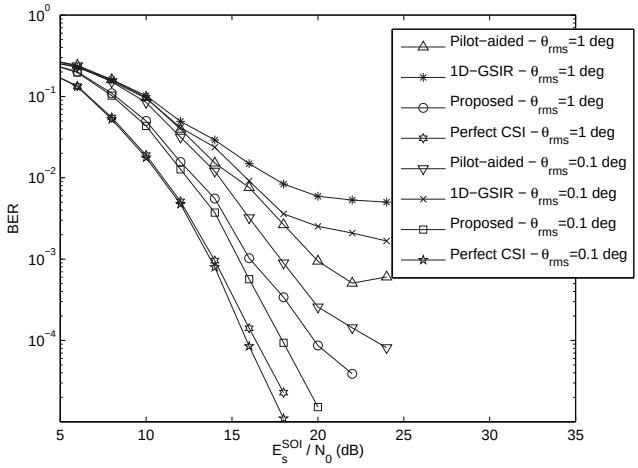

Fig. 5. BER using 16-QAM modulation under varying phase noise level for the pilot-aided, 1D-GSIR, proposed and perfect CSI methods after 3 iterations ($f_m/f_s = 5 \times 10^{-6}$).

distributed extrinsic symbol probabilities at the decoder output. Moreover, at instant $k = 0$, initial (resp. at instant $k = K$, final) Gaussian messages for the forward (resp. backward) pass on the CFR estimation subgraph, are obtained from Kalman smoothing in the subcarrier domain performed on the pilot OFDM blocks (see Fig. 2).

IV. Simulation results

Each frame contains $K = 60$ OFDM data blocks using memory-6 convolutional encoding with generators $(171, 131)$ in octal. Our OFDM setup adopts some essential values of the 802.11g standard [12], with sampling frequency $f_s = 20$ MHz, $N = 64$ subcarriers and $\Delta = 8$ samples. The phase noise standard deviation at the transmitter and receiver, θ_{rms}, corresponds to a phase-locked loop with 3 dB bandwidth $\Omega_0 = 100$ kHz [13]. Rapp's model [14], with parameters $\nu = 1$, $A_0 = 1$, $p = 3$ is used to simulate the PA, leading to $Q = 1$. The PA output back-off (OBO) is chosen as 4.92 dB so that the signal-to-3rd order nonlinearity power ratio is 20 dB. The CIRs $\mathbf{h}^{\mathsf{RSI}}(k)$ and $\mathbf{h}^{\mathsf{SOI}}(k)$ are simulated according to a Rayleigh fading model with an exponentially decreasing power delay profile that has a decay constant of three taps. Jakes' Doppler power spectrum is assumed, with maximum Doppler shift f_m (in Hertz). After both passive and active analog SI suppression, the RSI-to-SOI power ratio is set to $10\log 10(E_s^{\mathsf{RSI}}/E_s^{\mathsf{SOI}}) = 10$ dB. The following algorithms were employed at the $\mathsf{N}^{\mathsf{RSI}}$ receiver:

1) **Proposed**: the proposed iterative receiver in Sec. III
2) **Perfect CSI**: the proposed receiver with perfect channel state information (CSI)
3) **Pilot-aided**: after removing the SOI estimate we first jointly estimate $\mathbf{c}^{\mathsf{RSI}}(k)$ and $\mathbf{g}^{\mathsf{RSI}}(k)$ using the LS method in [3] on pilot blocks. On data blocks, $\mathbf{c}^{\mathsf{RSI}}(k)$ and $\mathbf{g}^{\mathsf{RSI}}(k)$ are obtained by temporal interpolation. Then, after RSI removal in the time domain, we apply the proposed method by removing the two first coordinates from the channel state $\mathbf{x}_n(k)$ in (7)
4) **1D-GSIR**: the graph-based soft iterative receiver (GSIR) in [9]. For the sake of fair comparison with the proposed scheme in terms of complexity, channel variations are considered in the time domain only (1D).

An EXIT analysis [15] for the three first receivers based on our method (not included due to lack of space) shows that $\zeta = 10$ is a near-optimal choice for the hyperparameters in (9). Regarding 1D-GSIR, ζ is set to 1 as specified in [9].

Fig. 4 shows the bit error rate (BER) for 4-QAM modulation with $\theta_{rms} = 1\,\mathrm{deg}$, for different values of normalized fading rate, f_m/f_s. At convergence, both iterative receivers (Proposed and 1D-GSIR) outperform the pilot-aided receiver thanks to code-aided re-estimation of both the linear and nonlinear part of the time-varying channel on each OFDM data block. Fig. 5 shows the BER for 16-QAM modulation with $f_m/f_s = 5 \times 10^{-6}$, for different values of θ_{rms}. As expected, phase noise generates additional unmodeled ICI, which ultimately becomes the limiting factor for low-cost local oscillators at high signal-to-noise ratio (even more so when the RSI-to-SOI power ratio is raised to 15 dB). Also note that the proposed method outperforms 1D-GSIR, especially for 16-QAM. This result can be interpreted as a consequence of using a different Gaussian approximation and the inability of 1D-GSIR to estimate jointly the CFR parameters.

V. Conclusion

In this paper, we proposed a message-passing algorithm suitable for joint channel estimation, RSI cancellation, symbol detection and decoding for FD OFDM transmissions. We derived a low-cost iterative receiver by exploiting per-subcarrier processing and message parameterization with Gaussian densities. Performances are close to the perfect CSI case, even for low pilot overhead and rapid temporal channel variations. In future work, we will focus on factor graph-based ICI modeling and compensation of the far-end frequency offset and phase noise. Extensions of the present work to single-carrier and (multiple-input multiple-output) MIMO full-duplex systems is yet another open problem.

REFERENCES

[1] D. Kim, H. Lee and D. Hong, "A survey of in-band full-duplex transmission: from the perspective of PHY and MAC layers," *IEEE Communication Surveys & Tutorials*, vol. 17, no. 4, pp. 2017-2046, Fourth Quarter, 2015.

[2] S. Li and R.D. Murch, "Full-duplex wireless communication using transmitter output based echo cancellation," *Proc. IEEE GLOBECOM 11*, pp. 1-5, Houston, TX, USA, Dec. 2011.

[3] L. Anttila, D. Korpi, V. Syrjälä, and M. Valkama, "Cancellation of power amplifier induced nonlinear self-interference in full-duplex transceivers," *Proc. 47th Asilomar Conference on Signals, Systems and Computers*, pp. 1193-1198, Nov. 2013.

[4] M. Jain, J.I. Choi, T.M. Kim, D. Bharadia, S. Seth, K. Srinivasan, P. Levis, S. Katti and P. Sinha, "Practical, real-time, full duplex wireless," *Proc. ACM MobiCom 11*, pp. 301-312, Las Vegas, NV, USA, Sept. 2011.

[5] E. Ahmed, and A.M. Eltawil, "All-digital self-interference cancellation technique for full-duplex systems," *IEEE Trans. Wir. Communications*, vol. 14, no. 7, pp. 3519-3532, Jul. 2015.

[6] X. Zhang, W. Cheng and H. Zhang, "Full-duplex transmission in PHY and MAC layers for 5G mobile wireless networks", *IEEE Wireless Communications*, vol. 22, Iss. 5, pp. 112-121, Oct. 2015.

[7] A. Sahai, G. Patel, C. Dick and A. Sabharwal, "On the impact of phase noise on active cancellation in wireless full-duplex", *IEEE Trans. Veh. Technol.*, pp. 4494-4510, vol. 62, no. 9, Nov. 2013.

[8] V.A. Bohara and S.H. Ting, "Analytical performance of frequency division multiplexing systems impaired by a non-linear high-power amplifier with memory", *IET Commun.*, pp. 1659-1666, vol. 3, Iss. 10, 2009.

[9] C. Knievel, P. A. Hoeher, A. Tyrrell, and G. Auer, "Multi-dimensional graph-based soft iterative receiver for MIMO-OFDM," *IEEE Trans. Commun.*, vol. 60, no. 6, pp. 1599-1606, June 2012.

[10] H.-A. Loeliger, "An introduction to factor graphs," *IEEE Sig. Proc. Mag.*, pp. 28-41, vol. 21, no. 1, Jan. 2004.

[11] L.R. Bahl, J. Cocke, F. Jelinek and J. Raviv, "Optimal decoding of linear codes for minimizing symbol error rate," *IEEE Trans. Inform. Theory*, Vol. 20, pp. 284-287, March 1974.

[12] IEEE Standard 802.11g-2003, Part 11: Wireless LAN Medium Access Control (MAC) and Physical Layer (PHY) Specifications - Amendment 4: Further Higher Data Rate Extension in the 2.4 GHz Band, IEEE, 2003.

[13] D.D. Lin, R.A. Pacheco, T.J. Lim and D. Hatzinakos, "Joint estimation of channel response, frequency offset, and phase noise in OFDM," *IEEE Trans. Sig. Proc.*, pp. 3542-3554, vol. 54, no. 9, Sept. 2006.

[14] C. Rapp, "Effects of the HPA-nonlinearity on a 4-DPSK/OFDM signal for a digital sound broadcasting system," *Proc. Second European Conf. on Sat. Comm.*, pp. 179-184, Liege, Belgium, Oct. 1991.

[15] S. ten Brink, "Convergence behavior of iteratively decoded parallel concatenated codes," *IEEE Trans. Comm.*, vol. 49, no. 10, pp. 1727-1737, Oct. 2001.